Uncovering reflection insensitive semiconductor lasers for silicon photonic integration

Frédéric Grillot
LTCI, Télécom Paris, Institut Polytechnique de Paris, 19, place Marguerite Perey, 91120 Palaiseau, France.

Center for High Technology Materials, University of New Mexico, Albuquerque, NM 87106 USA
frederic.grillot@telecom-paris.fr

Abstract: We report on two recent high performance semiconductor lasers made with the silicon photonic platform. Both structures display a quasi complete reflection insensitivity, resulting in a key attribute for the development of isolator-free integrated technologies.

OCIS codes: 250.5960, 140.3490, 250.5590.

1. Introduction

The development of on-chip photonic integration brings together many innovative perspectives and approaches for high-speed communication systems, optical interconnects, board-to-board and chip-to-chip integrated circuits. In photonics integrated circuits (PIC), unwanted reflections are known to be problematic to maintain a stable laser operation [1]. External optical feedback (EOF) can have a major impact on the performance of semiconductor lasers. Among the large variety of potential effects, whose presence depends on the external cavity length and EOF strength, coherence collapse (CC) is the most influential and penalizing factor affecting the stability and purity of the device [2]. This effect is even more detrimental in PICs because light emitters are tightly assembled with other optical components (eg., modulators, waveguides, etc.) to achieve the desired functionality hence resulting in possible optical reflections on the silicon integrated devices. To overcome this problem, an optical isolator is inserted to block the feedback light back into the active region and to avoid potential laser unstabilities. However, optical isolators are cost prohibited because they can often exceed the cost of the laser chip itself. In addition, chip-scale integration of low-loss and sufficient isolation ratio optical isolators into photonic circuits is not yet available. Therefore, the development of feedback insensitive lasers remains a major objective for silicon photonic integration required to alleviate the risk of undesired reflections. A very interesting pioneer study was reported on an InAs/GaAs quantum dot (QD) transmitter integrated on silicon operating without optical isolator for core I/O applications [3] demonstrating significant advances in the field. Other accomplishments include semiconductor lasers with an intracavity optical isolator [4], photonics crystal Fano nanolasers [5], and parity-time symmetry distributed feedback (DFB) lasers [6] among many others. However, despite the progress demonstrated up-to-date, a light source with absolute feedback insensitivity has yet to be reported particularly down to the system level. In this work, we shed insight on two recent demonstrations exhibiting a quasi complete reflection insensitivity. The first device is a hybrid III-V on silicon DFB laser with a large quality factor (eg., Q-factor) [8] whereas the second is an epitaxial Fabry-Perot QD laser on silicon [9]. Both devices are made with the silicon photonic platform. They are compact, cost-efficient and exhibit 10 Gbps error-free transmissions under strong optical feedback demonstrating that the relative intensity noise of each laser, which is associated to the noise power received at the photodiode is not affected by EOF. In the end, this work shows the possibility to integrate such devices with other components without the high cost imposed by the need of an optical isolator.

2. Directions for reflection insensitivity

The sensitivity to EOF can be analyzed from the coupling coefficient X given by [2],

$$X = \omega \tau_{ext} Q^{-1} \sqrt{r_{ext}} \sqrt{1+\alpha_H^2} \tag{1}$$

with τ_{ext} the external roundtrip time, α_H the so-called linewidth enhancement factor, r_{ext} the feedback strength defined as the ratio between the reflected power and free-space emitting power at the front facet whereas $Q = \omega\tau_p = \omega/v_g\alpha$ is the Q of the cavity with v_g the group velocity, α the total loss and τ_p the cavity photon lifetime. Eq. (1) tells us that large values of X increase the number of external cavity modes giving rise to modal competition and possible laser instabilities [2].

In addition to (1), the maximum feedback ratio that can be practically tolerated for a stable laser operation into a communication system is given from the critical feedback level r_{crit} such as [2]

$$r_{crit} = \frac{\tau_l^2 \gamma^2}{16 C_k^2} \left(\frac{1+\alpha_H^2}{\alpha_H^4} \right) \tag{2}$$

with τ_l the photon roundtrip time in the laser cavity, γ the damping factor, and C_k the external coupling coefficient of the facet ($k = r,l$ for rear (r) or front (l)) defined such as $C_k = \frac{j\tau_{in}}{2}\left(1-r_k^2\right)\frac{\partial \hat{W}/\partial r_k}{\partial \hat{W}/\partial \omega}$ with r_k the amplitude reflectivity, and $\hat{W}$ the Wronskian operator whose expression depends on the type of semiconductor laser under consideration [7]. The critical feedback level describes the undamping of the relaxation oscillations which further degenerates into the coherence collapse (CC) regime where the relative intensity noise (RIN) of the laser is drastically enhanced. Together, (1) and (2) can be used to unlock feedback insensitive lasers. This can be performed by i.) minimizing the α_H-factor, ii.) increasing the damping factor γ, or iii.) having a large Q that is to say a low-loss laser with a long photon lifetime. In such way, both r_{crit} and X can be adjusted to the desired values thus providing a relative or complete feedback insensitivity regardless of the feedback strength. To reach these goals, the silicon photonic platform can be leveraged to our benefits at low-cost. In what follows, the reflection insensitivity of both devices is evaluated by using a fiberized transmission test-bed environment. Test-bed experiments are performed with a Mach-Zehnder modulator (MZM) at 10 Gbps (on-off keying) with a pseudo-random binary sequence (PRBS) and a bit sequence length of $2^{31}-1$. Afterwards, the modulated signal is pre-amplified and transmitted through a single-mode fiber (SMF). At the end, a variable optical attenuator (VOA) is used to tune the received power of the error detector in order to characterize the bit-error-rate (BER) performance.

3. Hybrid III-V/Si DFB laser

Fig. 1(a) sketches the cross section of the high-Q laser structure, associating a silicon photonic layer to a quantum well (QW) gain material. The geometry is optimized such that the mode is buried into a rib silicon waveguide with a shallow grating of 30 nm deep teeth. The width of the grating is tapered longitudinally to create an effective confining potential which allows a single, bell-shaped longitudinal mode within the stop band of the DFB. Depending on the silicon waveguide width W_{Si}, light can be either quasi-totally confined in the III-V or in the silicon waveguide. The Q is maximized by increasing the device length up to 900 microns hence leading to a large grating coupling coefficient at the center of the cavity of about 200 cm^{-1}. The Q factor is expected to be up to 10^6 which transforms into a long cavity photon lifetime of about $\sim$ 100 ps [8]. Fig. 1(b) shows the light-current (LI) characteristics. The threshold current I_{th} measured at room temperature is of 40 mA whereas the optical spectrum (inset) displays a single mode behavior with a side-mode suppression ratio (SMSR) beyond 50 dB at 3 $\times I_{th}$ along with an emission wavelength at 1562.6 nm.

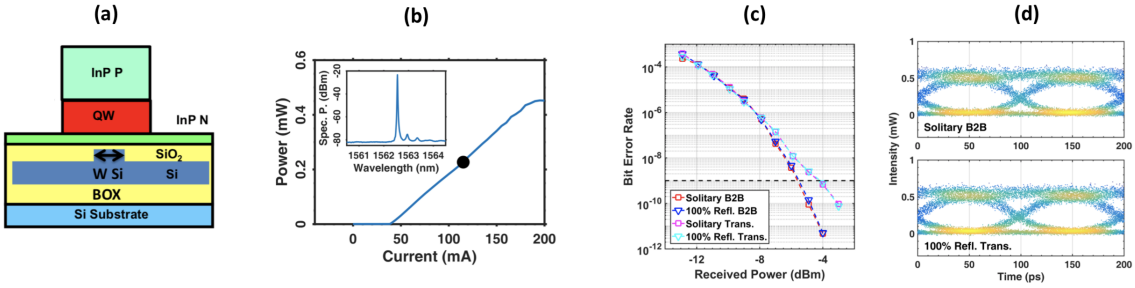

Fig. 1. (a) Transverse cross-section; (b) LI curve and optical spectrum (inset) at 3 $\times I_{th}$ (c) BER plots with (blue / cyan triangles) and without (red / magenta squares) feedback; (d) Eye diagrams in B2B without feedback (top) and with maximal feedback after transmission (down).

Fig. 1(c) depicts the BER characteristics for the back-to-back (B2B) and after propagation (10 km). In each case, the reference curve corresponds to the solitary case that is to say the situation without EOF (r_{ext}=0) while that with feedback is performed under the most stringent conditions ie., 100% of light back to the cavity. Overall, the high Q laser is highly resilient to external reflections leading to an error-free operation with BER as low as 10^{-12} (B2B) and 10^{-10} (after propagation), and with a power penalty of $\sim$ 1.5 dB that is only induced by the fiber chromatic dispersion. Fig. 1(d) displays the eye diagrams for the B2B without feedback (top) and after propagation with maximum feedback (down). Both remain clean and well-opened. Here, we demonstrate that the high Q can prevent any degradation of the laser's performance without exhibiting any CC regime operation.

4. Epitaxial QD lasers on silicon

As the drawbacks of heterogeneous integration includes the high cost and the limited scalability, direct epitaxial growth of III-V materials on silicon are also developed. To this end, epitaxial QD lasers on silicon have demonstrated record performance with threshold currents not exceeding a few milliamps, continuous wave operation up to 105°C, and very long device lifetime [9]. Fig. 2(a) shows the transverse cross-section of the Fabry-Perot laser under study incorporating 5 QD layers embedded into the active region. The threshold current I_{th} measured at room temperature is of 6 mA whereas the optical spectrum (inset) displays an emission wavelength at the fundamental transition close to 1305 nm. As previously, Fig. 2(c)(d) depict the BER characteristics and the eye diagrams for the B2B and after propagation (2 km). In each case, the solitary curve still corresponds to the situation without EOF while that with feedback assumes 100% of light back to the cavity. Overall, the epitaxial QD laser on silicon is found totally reflection insensitive with an error-free down to 10^{-12} thus demonstrating its strong potential as also confirmed by the eye diagrams shown in Fig. 2(d). The very high degree of feedback tolerance of the QD gain medium is highly dependent on the inhomogeneous broadening due to nanostructure size variations, but through careful optimization, it is possible to show that even epitaxial lasers on silicon display high performance for isolator-free photonic integration [9]. Such a remarkable feature leads to a near zero α_H-factor at threshold of ~ 0.3 and to the absence of higher energy states in the lasing emission even at high bias. Together these features combined with the large damping ($\sim$ 33 GHz) are linked to the critical feedback level and for this reason, one can classify these lasers as reflection insensitive when compared to the state-of-the-art commercial QWs [10].

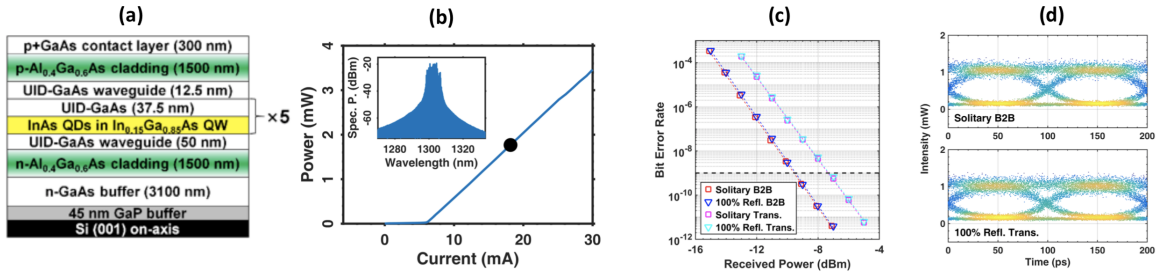

Fig. 2. (a) Transverse cross-section; (b) LI curve and optical spectrum (inset) at 3 $\times I_{th}$; (c) BER plots with (blue / cyan triangles) and without (red / magenta squares) optical feedback; (d) Eye diagrams in B2B without feedback (top) and with maximal feedback after transmission (down).

5. Conclusions

This work provides novel insights for designing high performance reflection insensitive semiconductor lasers, withstanding feedback rates much above the requirement dictated by the IEEE 802.3. As silicon photonics components are made in a CMOS fab, these results show the possibility to integrate lasers and other optical components without invoking the need of an optical isolator. Other applications requiring improved coherence and precisely controlled light sources will also benefit from these distinctive attributes and be considered in future developments.

The author acknowledges Prof. J. E. Bowers from the University of California Santa Barbara, Dr. A. de Rossi from Thales Research and Technology, and Dr. A. Shen from Nokia Bell Labs. Special thanks to S. Gomez and H. Huang for fruitful discussions.

References

1. Z. Zhang et al., IEEE J. Sel. Top. Quantum Electron., **25**, p. 1900509 (2019).
2. D. M. Kane & K. A. Shore, John Wiley & Sons, Ltd. (2005).
3. K. Mizutani et al., In the International Conference on Group IV Photonics, paper ThF3, p. 177 (2015).
4. D. Lenstra et al., IEEE J. Sel. Top. Quantum Electron., **25**, p. 1502113 (2019).
5. T. S. Rasmussen et al., In ArXiv preprint arXiv:1906.06923 (2019).
6. V. Brac de la Perrière et al., Proc. SPIE, Integrated Optics: Physics and Simulations III, **10242C** (2017).
7. F. Grillot et al., IEEE J. of Quantum Electron., **40**, p. 231 (2003).
8. A. Gallet et al., IEEE International Semiconductor Laser Conference (ISLC), p. 45 (2018).
9. J. C. Norman et al., IEEE J. of Quantum Electron., **55**, p. 2001111 (2019).
10. J. Duan et al., IEEE Photon. Technol. Letts, **31**, p. 345 (2019).